

Supplementary Materials

Experimental Section

Materials

Titanium tetrachloride(TiCl_4 , 99.9%), Tetrabutyl titanate (98%) were acquired from Sinopharm Chemical Reagent Co., Ltd. Methylammonium Chloride(MACl , $\geq 99.5\%$), methylammonium bromide (MABr , $\geq 99.5\%$), Methylammonium Iodide(MAI , $\geq 99.5\%$) were purchased from Xi'an Polymer Light Technology Corp. Caesium bromide (CsBr , 99.5%), Silver bromide (AgBr , 98%), Bismuth(III) bromide (BiBr_3 , $\geq 98\%$), dimethylsulfoxide (DMSO) and chlorobenzene (CB) were obtained from Macklin. All chemicals were used without further purification.

Device fabrication

The TiO_2 dense layer was obtained by thermal deposition at 70°C in water bath with 0.1M TiCl_4 solution. After annealing at 450°C , it was put into the tank of the reaction kettle containing tetrabutyl titanate solution to react with 110 minutes. TiO_2 nanorods were prepared by annealing at 450°C for 30 minutes. The concentration of $\text{Cs}_2\text{AgBiBr}_6$ precursor solution is 0.5M. CsBr , AgBr and BiBr_3 were added to DMSO at a molar mass of 2:1:1 and stirred at 70°C for more than 10 hours. Double perovskite precursor solution was obtained after filtration. The FTO/ TiO_2 substrate was preheated to 10 minutes at 70°C and then spin-cast by perovskite precursor solution followed by spin-coating of antisolvent CB. After annealing at 280°C for 10 minutes, $\text{Cs}_2\text{AgBiBr}_6$ perovskite films were obtained. As for $\text{Cs}_2\text{AgBiBr}_6$ -MAX, MAX solution was spin-cast before spin-coating of perovskite precursor solution. The concentration ratio of perovskite precursor/MAX is set at 2:1. After finishing the growth of

TiO₂ NRs, 0.25M-MAX solution was spin-coated in advance on the TiO₂ ETL followed by spin-coating Cs₂AgBiBr₆ precursor. 0.25mmol MAcl, MABr and MAI were dissolved separately in DMSO to prepare MAX solution. The entire preparation procedure of Cs₂AgBiBr₆ film was carried out in airing chamber. The low temperature carbon paste was coated on the perovskite layer by screen printing, and heat-treated at 100°C for 10 minutes to obtain carbon based electrode. The active area of the device is ~0.06cm².

Characterization

Crystalline structures were tested by an X-Ray Diffractometer (XRD, Brucker D8). The top-view and cross-sectional morphologies were investigated by SEM (JEOL JSM-7100F). The chemical bonding was recorded by XPS spectrometer (Thermo scientific, ESCALab 250xi). The absorption curves were collected by a UV–vis-NIR spectrophotometer (UV-3600, Shimadzu). The photoluminescence spectroscopy measurements were measured with a fluorescence spectrophotometer (FLS 1000). The Fourier transform infrared (FTIR) spectra were obtained by Vacuum Fourier Transform Infrared Spectroscopy of Brooke Company in Germany (VERTEX 70v). The J-V curves of PeSCs were finished with the American Newport Oriol test system (forward scan parameters: 1.5V to 0V, step length 0.02V; reverse scan parameters: 0V to 1.5V, step length 0.02V). The sunlight intensity was calibrated with a certified reference silicon solar cell. The EQE was measured by Keithley 2400 source meter and solar simulator (Newport 67005) under standard AM 1.5G illumination. The EIS measurement was conducted by an electrochemical station (CHI760e).

Supporting tables

Table S1 PL decay parameters of TiO₂/ Cs₂AgBiBr₆ films.

Samples	A ₁	τ ₁ (ns)	A ₂	τ ₂ (ns)	τ
Reference	0.996	45.83	0.035	166.34	59.46
MACl	0.699	1.74	0.281	46.34	42.53
MABr	0.530	3.25	0.402	52.25	48.53
MAI	0.646	2.43	0.359	48.81	45.00

TRPL spectra of TiO₂/ Cs₂AgBiBr₆ films were fitted by the following formula^[1].

$$y = y_0 + A_1 e^{-\left(\frac{x}{\tau_1}\right)} + A_2 e^{-\left(\frac{x}{\tau_2}\right)} \quad (1)$$

Where τ₁ and τ₂ are the fast decay time related to defects and slow decay time related to bimolecular recombination, respectively, and A₁ and A₂ are amplitudes. The carrier recombination lifetime (τ) was calculated by the formula:

$$\tau = \frac{A_1 \tau_1^2 + A_2 \tau_2^2}{A_1 \tau_1 + A_2 \tau_2} \quad (2)$$

Table S2 Photovoltaic parameters of the best Cs₂AgBiBr₆ PeSCs with and without MAX pre-treatment.

Cs₂AgBiBr₆ Samples	Voc (V)	Jsc(mA cm⁻²)	FF (%)	PCE (%)	HI
FW	1.10	2.17	45	1.08	
Reference RE	1.06	2.29	50	1.20	0.17
Ave.	1.05±0.05	1.92±0.44	46±5.48	1.01±0.19	
FW	1.09	3.05	59	1.96	
MACl RE	1.07	3.04	62	2.03	0.05
Ave.	1.06±0.05	2.94±0.11	60±3.43	1.92±0.11	
FW	1.06	2.34	59	1.46	
MABr RE	1.01	2.57	59	1.55	0.12
Ave.	1.07±0.06	2.29±0.25	53±6.97	1.34±0.21	
FW	1.05	2.51	62	1.66	
MAI RE	1.03	2.79	63	1.80	0.11
Ave.	1.08±0.07	2.66±0.14	59±4.18	1.51±0.29	

Table S3 Rs, Rct and C fitted by nyquist EIS diagram.

Sample	Rs(KΩ)	Rct(KΩ)	C(F)
Reference	76.34	1.993	4.004E-8
MACl	70.05	1.272	2.940E-8
MABr	71.23	1.507	5.275E-9
MAI	71.78	1.360	4.242E-8

Table S4 Rsh, Rs and J₀ derived from dark J-V curves

Sample	Rsh($\Omega \text{ cm}^2$)	Rs($\Omega \text{ cm}^2$)	lnJ ₀	J ₀ (mA cm ⁻²)
Reference	7.07E7	71.38	-10.41	3.01E-5
MACl	6.85E6	94.76	-13.60	1.24E-6
MABr	2.06E6	92.69	-11.40	1.12E-5
MAI	1.60E6	84.47	-12.47	3.84E-6

The dark current fitting of the device was according to the following formula ^[2, 3].

$$-\frac{dV}{dJ} = \frac{AK_B T}{e} \frac{1}{(J_{sc} - J)} + R_s \quad (3)$$

$$\ln(J_{sc} - J) = \frac{e}{AK_B T}(V + R_s * J) + \ln J_0 \quad (4)$$

Here A is the ideal factors of the diode, R_S is the series resistance, R_{SH} is the shunt resistance, and J₀ reverse saturation current. K_B is the Boltzmann constant, T is the absolute temperature, e is the basic charge, and V is the DC bias voltage applied to the cell.

Table S5 Photovoltaic parameters of the champion devices stored within 30 days.

Samples	Days	V _{oc} (V)	J _{sc} (mA cm ⁻²)	FF (%)	PCE (%)
Reference	0	1.06	2.29	50	1.20
	5	1.07	2.26	49	1.19
	10	1.08	2.23	47	1.12
	15	1.09	2.23	46	1.12
	20	1.10	2.17	46	1.10
	30	1.19	1.89	44	1.00
	MACl	0	1.07	3.04	62
5		1.09	2.99	61	2.01
10		1.15	2.99	58	2.00
15		1.13	3.00	58	1.97
20		1.13	2.98	57	1.93
30		1.22	2.61	58	1.85

Supporting Figures

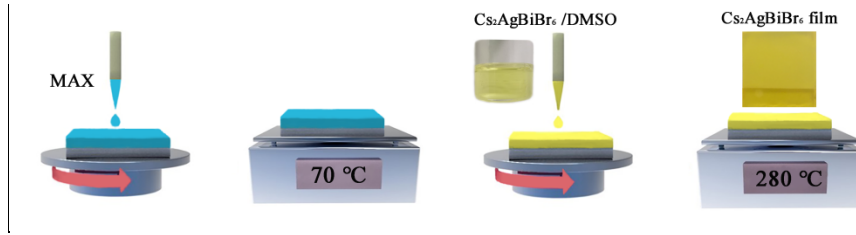


Fig.S1 (a) Diagrammatic sketch for preparation process of $\text{Cs}_2\text{AgBiBr}_6$ films with MAX pre-treatment (X is Cl^- , Br^- and I^-).

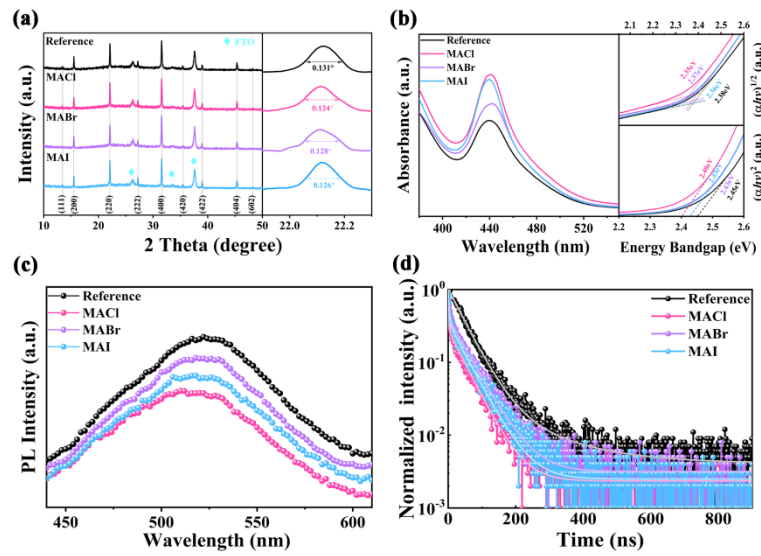


Fig. S2 (a) XRD patterns and (220) diffraction peaks of perovskite films. The FWHM value is measured for (220) plane. (b) UV-vis absorption spectra of $\text{Cs}_2\text{AgBiBr}_6$ perovskite films. (c) PL and (d)TRPL spectra of $\text{Cs}_2\text{AgBiBr}_6$ perovskite films.

The bandgap of $\text{Cs}_2\text{AgBiBr}_6$ films was determined by Tauc curve equation.

$$(\alpha h\nu)^{1/n} = A(h\nu - E_g) \quad (1)$$

Where α represents the absorption coefficient, h is the Planck constant and ν is the incident frequency, A is a proportional constant [4, 5].

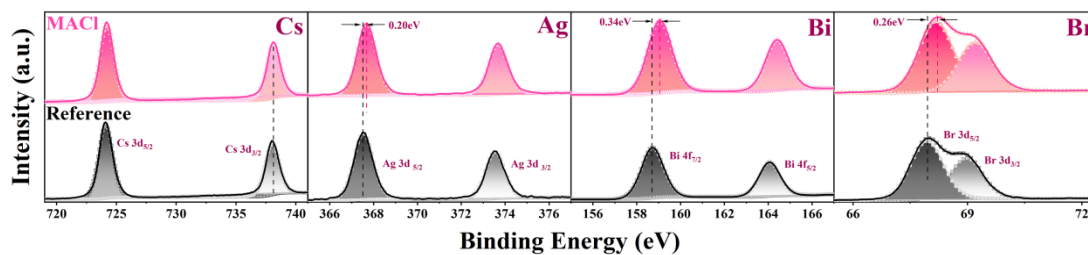


Fig. S3 XPS spectra of Cs 3d, Ag 3d, Bi 4f and Br 3d in reference films treated and $\text{Cs}_2\text{AgBiBr}_6$ -MACl films.

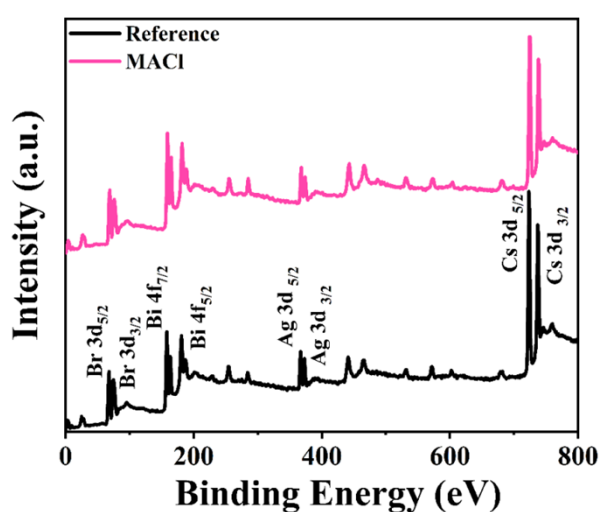


Fig.S4 Survey X-ray photoelectron spectroscopy (XPS) spectra of the reference and $\text{Cs}_2\text{AgBiBr}_6$ -MACl.

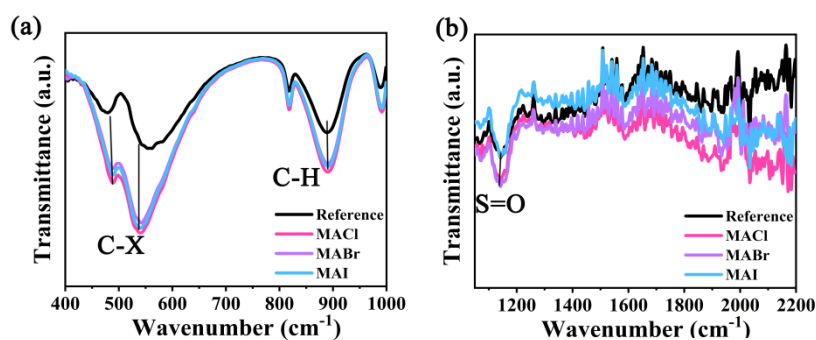


Fig.S5 Fourier transform infrared spectrometer (FT-IR) spectra of $\text{Cs}_2\text{AgBiBr}_6$ samples

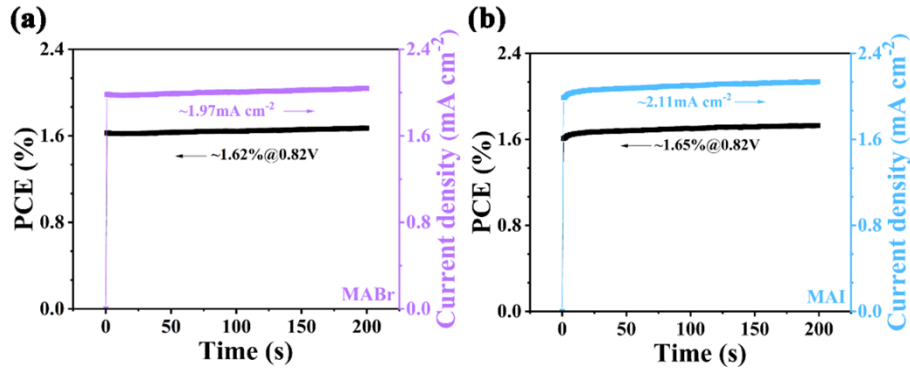


Fig.S6 Steady-state power outputs at the maximum power point of (a) $\text{Cs}_2\text{AgBiBr}_6\text{-MABr}$ and (b) $\text{Cs}_2\text{AgBiBr}_6\text{-MAI}$.

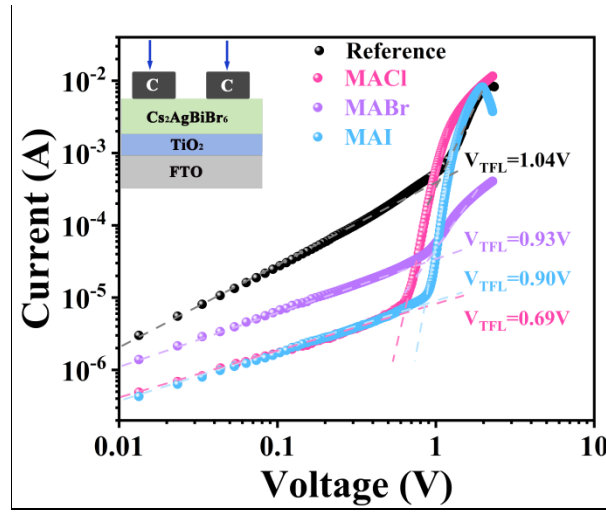


Fig.S7 Schematic diagram and dark I-V curves of $\text{Cs}_2\text{AgBiBr}_6$ devices.

The space-charge limited current (SCLC) model was used to calculate the trap density (N_{trap}).

$$N_{t r} \bar{a} \frac{2 \epsilon_0 V_{T F L}}{e L^2} \quad (5)$$

Where e , L , ϵ and ϵ_0 are the basic charge, the thickness of the active layer, the relative permittivity of $\text{Cs}_2\text{AgBiBr}_6$ and the vacuum dielectric constant ($8.8542 \times 10^{-14} \text{ F/cm}$), respectively.^[6, 7] The trap-filled limit voltage (V_{TFL}) was 1.04V, 0.69V, 0.93V and 0.90V, producing N_{trap} was $1.468 \times 10^{15} \text{ cm}^{-3}$, $9.737 \times 10^{14} \text{ cm}^{-3}$, $1.312 \times 10^{15} \text{ cm}^{-3}$ and $1.27 \times 10^{15} \text{ cm}^{-3}$ for the reference $\text{Cs}_2\text{AgBiBr}_6$, $\text{Cs}_2\text{AgBiBr}_6\text{-MAI}$, $\text{Cs}_2\text{AgBiBr}_6\text{-MABr}$ and $\text{Cs}_2\text{AgBiBr}_6\text{-MAI}$ devices, respectively.

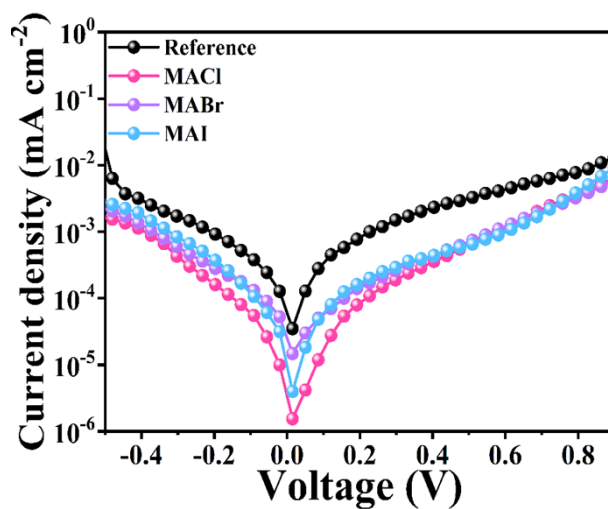


Fig.S8 J-V curves of $\text{Cs}_2\text{AgBiBr}_6$ PeSCs in dark.

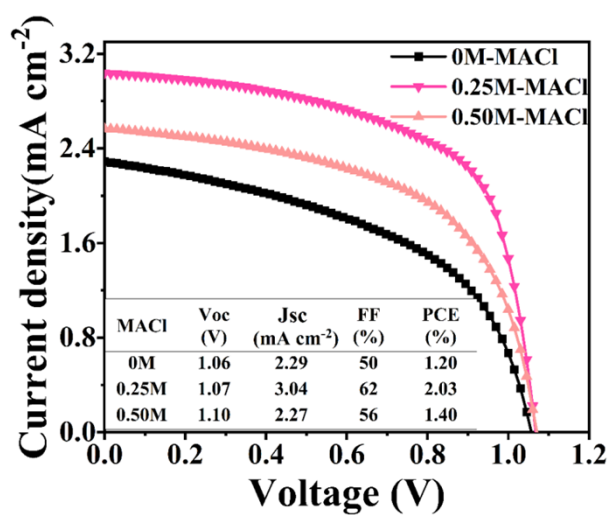


Fig.S9 J-V curves of $\text{Cs}_2\text{AgBiBr}_6$ devices pre-treated with different concentration MACl.

References

1. Y. Han, H. Zhao, C. Duan, S. Yang, Z. Yang, Z. Liu and S. Liu, *Adv. Funct. Mater.*, 2020, **30**,

- 1909972.
2. P. Liao, X. Zhao, G. Li, Y. Shen and M. Wang, *Nanomicro. Lett.*, 2018, **10**, 5.
 3. J. Shi, J. Dong, S. Lv, Y. Xu, L. Zhu, J. Xiao, X. Xu, H. Wu, D. Li, Y. Luo and Q. Meng, *Appl. Phys. Lett.*, 2014, **104**, 063901.
 4. B. D. Viezbicke, S. Patel, B. E. Davis and D. P. Birnie, *Phys. Status Solidi B*, 2015, 252, 1700-1710.
 5. P. Hou, W. Yang, N. Wan, Z. Fang, J. Zheng, M. Shang, D. Fu, Z. Yang and W. Yang, *J. Mater. Chem. C*, 2021, 9, 9659-9669.
 6. Z. Shuang, H. Zhou, D. Wu, X. Zhang, B. Xiao, G. Ma, J. Zhang and H. Wang, *Chem. Eng. J.*, 2022, **433**, 063901.
 7. H. Wu, Y. Wang, A. Liu, J. Wang, B. J. Kim, Y. Liu, Y. Fang, X. Zhang, G. Boschloo and E. M. J. Johansson, *Adv. Funct. Mater.*, 2021, 32, 2109402.